

Electronic Structure and Optical Properties of AFeO₂ (A = Ag, Cu) within GGA Calculations

Khuong P. Ong,[†] Kewu Bai,[†] Peter Blaha,[‡] and Ping Wu^{*,†}

Institute of High Performance Computing, 1 Science Park Road, #01-01 The Capricorn Singapore Science Park II, Singapore 117528, and Institute for Materials Chemistry, Vienna University of Technology, A-1060 Vienna, Austria

Received October 17, 2006. Revised Manuscript Received November 21, 2006

The electronic structure of delafossite type oxides AFeO₂ (A = Ag, Cu) has been calculated using the full potential linearized augmented plane wave (FP-LAPW) method within the local spin density approximation (LSDA), Perdew–Burke–Ernzerhof (PBE-GGA), and Engel–Vosko (EV-GGA) generalized-gradient approximations. It was found that the EV-GGA provides a more realistic description of the electronic structure and the optical properties of AFeO₂ than PBE-GGA or LSDA. The influence of electron correlations has been considered within the PBE-GGA+*U* and LSDA+*U* methods. The effective Hubbard *U*, *U*_{eff}, has been derived on the basis of an ab initio constraint calculation and by comparison with X-ray emission spectra. The energy band gap of AFeO₂ within the PBE-GGA+*U* is found as a charge-transfer gap between O-2p to Fe-3d states. The theoretical optical band gaps Δ₀ = 1.30, Δ₁ = 2.06, and Δ₂ = 3.20 eV for CuFeO₂ are quite compatible with experimental data. We have predicted an optical band gap Δ₀ = 1.90 eV for AgFeO₂, and the increase in the optical and energy band gaps of AgFeO₂ in comparison with CuFeO₂ can be understood as a size effect.

I. Introduction

Layered structures with dumbbell O–A–O layers and octahedral BO₆ layers stacked along the *c*-axis of delafossite type oxides ABO₂ (A = Ag, Pd, Cu, Pt; B = Sc, Cr, Fe, Co, Ni, Rh) have been attracting much attention because of physical properties related to this structure,^{1–9} e.g., the electrical conductivity in the A- plane is much higher than that along the *c*-axis,³ frustrated magnetic properties in the BO₂ layer due to the triangular lattice,^{4,5} high optical band gap in CuAlO₂,^{6,7} CuGaO₂,⁸ CuInO₂,⁹ etc. Most of the delafossite oxides are semiconductors; some of them are metals, e.g., PdCoO₂, PtCoO₂, PtRhO₂, or semimetals, such as AgNiO₂. Delafossite materials are currently used as electrode materials in miniature batteries (AgNiO₂),¹⁰ functional windows (CuAlO₂),¹¹ catalysts, e.g., synthesis of methanol using CuCrO₂,¹² and conversion of toxic gases emanated by internal combustion engines using CuFeO₂.^{13,14}

Delafossite CuFeO₂ has been extensively investigated as material for quasi-two-dimensional frustrated magnetism.^{15–18} Its electronic structure has been studied by Galakhov et al.,¹⁹ within the LSDA and LSDA+*U* approach; LSDA calculations were performed using the full-potential linearized augmented plane wave method (FP-LAPW) as well as the linearized muffin-tin orbitals in the atomic sphere approximation (LMTO-ASA) method, whereas LSDA+*U* calculations were carried out using the LMTO-ASA method. However, the reported energy band gap, which is the gap between the top of the valance band and the bottom of the conduction band, is 2.0 eV, much larger than the optical band gap of 1.15 eV reported from experimental data.²⁰ The other two optical gaps of 2.03 and 3.35 eV²⁰ have not been clarified from a theoretical point of view. In addition, the reported partial densities of states (PDOS) of Cu, Fe, and O, with and without electron correlations, are incompatible with X-ray emission spectra.¹⁹

Having the same closed shell electronic configuration of the A-layer as CuFeO₂, AgFeO₂ is a semiconductor with two polytypes, rhombohedral (3R) and hexagonal (2H). The

- * Corresponding author. Email: wuping@ihpc.a-star.edu.sg.
[†] Institute of High Performance Computing.
[‡] Vienna University of Technology.
- (1) Shannon, R. D.; Rogers, D. B.; Prewitt, C. T. *Inorg. Chem.* **1971**, *10*, 713.
 - (2) Prewitt, C. T.; Shannon, R. D.; Rogers, D. B. *Inorg. Chem.* **1971**, *10*, 719.
 - (3) Rogers, D. B.; Shannon, R. D.; Prewitt, C. T.; Gillson, J. L. *Inorg. Chem.* **1971**, *10*, 723.
 - (4) Angelov, S.; Doumerc, J. P. *Solid State Commun.* **1991**, *77*, 213.
 - (5) Doumerc, J. P.; Wichainchai, A.; Ammar, A.; Pouchard, M.; Hagenmuller, P. *Mater. Res. Bull.* **1986**, *21*, 745.
 - (6) Benko, F. A.; Koffyberg, F. P. *J. Phys. Chem. Solids* **1984**, *45*, 57.
 - (7) Yanagi, H.; Inoue, S.; Ueda, K.; Kawazoe, H.; Hosono, H.; Hamada, N. *J. Appl. Phys.* **2000**, *88*, 4159.
 - (8) Ueda, K.; Hase, T.; Yanagi, H.; Kawazoe, H.; Hosono, H.; Ohta, H.; Orita, M.; Hirano, M. *J. Appl. Phys.* **2001**, *89*, 1790.
 - (9) Yanagi, H.; Hase, T.; Ibuki, S.; Ueda, K.; Hosono, H. *Appl. Phys. Lett.* **2001**, *78*, 1583.
 - (10) Ray-O-Vac Co. Japanese Kokai Tokkyo Koho 8277 645 756 757.
 - (11) Kawazoe, H.; Yasukawa, M.; Hyodo, H.; Kurita, M.; Yanagi, H.; Hosono, H. *Nature* **1997**, *389*, 939.

- (12) Monnier, J. R.; Hanrahan, M. J.; Apai, G. *J. Catal.* **1985**, *92*, 119.
- (13) Carreiro, L. *Mater. Res. Bull.* **1985**, *20*, 619.
- (14) Christopher, J.; Swamy, C. S. *J. Mater. Sci.* **1992**, *27*, 1353.
- (15) Ye, F.; Ren, Y.; Huang, Q.; Fernandez-Baca, J. A.; Dai, P.; Lynn, J.W.; Kimura, T. *Phys. Rev. B* **2006**, *73*, 220404.
- (16) Kimura, T.; Lashley, J. C.; Ramirez, A. P. *Phys. Rev. B* **2006**, *73*, 220401.
- (17) Terada, N.; Mitsuda, S.; Ohsumi, H.; Tajima, K. *J. Phys. Soc. Jpn.* **2006**, *75*, 23602.
- (18) Makata, M.; Yaguchi, N.; Takagi, T.; Sugino, T.; Mitsuda, S.; Yoshizawa, H.; Hotoito, N.; Shinjo, T. *J. Phys. Soc. Jpn.* **1993**, *62*, 4474.
- (19) Galakhov, V. R.; Poteryaev, A. I.; Kurmaev, E. Z.; Anisimov, V. I.; Bartkowski, S.; Neumann, M.; Lu, Z. W.; Klein, B. M.; Zhao, T. R. *Phys. Rev. B* **1997**, *56*, 4584.
- (20) Benko, F. A.; Koffyberg, F. P. *J. Phys. Chem. Solids* **1987**, *48*, 431.

electronic structures of 3R and 2H AgFeO₂ have been studied by Seshadri et al.,²¹ however, a metallic state instead of a true insulating state has been reported. So far, there have been no experimental reports on the energy band gap of this compound. Recently,²² we reported an energy band gap of 1.16 eV using the PBE-GGA+*U* method with a large $U_{\text{eff}} = 7.86$ eV. This energy band gap is nearly the same as the one reported for CuFeO₂²⁰ (1.15 eV). Optical experiments revealed that the energy band gap of CuMO₂ is less than that of AgMO₂ (with M = Al, Ga, In). Moreover, the electrical resistivity of AgFeO₂ was reported to be much larger than that of CuFeO₂.³ Therefore, we expect AgFeO₂ to have a larger energy band gap than CuFeO₂.

Nie, Wei, and Zhang²³ reported that the optical band gaps of delafossite CuAlO₂, CuAgO₂, and CuInO₂ are much larger than the energy band gaps because the dipole selection rules limit the allowed transitions between band edge states. In this work, the same phenomenon is observed for CuFeO₂ and AgFeO₂.

In this paper, we examine the electronic structure of AFeO₂ compounds within different approximations: LSDA, PBE-GGA, or EV-GGA,²⁴ with or without additional local correlation effects due to an effective Hubbard-*U*. These calculations aim to describe the semiconducting nature and the optical properties of AFeO₂ compounds in comparison with experiments. We considered a simple ferromagnetic order in the hexagonal phase, neglecting the 2D anti-ferromagnetic frustration observed at low temperatures and accompanied by structural phase transitions. To see the influence of electron correlations on the electronic structures of AFeO₂, we investigated the dependency of the energy band gap versus U_{eff} . To estimate the effect of on-site correlations on the ground state of CuFeO₂, X-ray emission spectra of CuFeO₂ have been studied within the EV-GGA, PBE-GGA, and PBE-GGA+*U* and compared with experimental results. From these calculations, a reasonable value of $U_{\text{eff}} = 2.18$ eV was extracted, which can then be used to study the electronic structure and optical properties of AFeO₂, leading to results that are consistent with those from the experiment. To this end, we present an analysis of the origin of the larger energy band gap in AgFeO₂ compared to CuFeO₂.

II. Computational Details

All calculations in this work were carried out with the Wien2k software package.²⁵ This program allows us to compute the electronic structure of AFeO₂ compounds within the density functional theory (DFT) applying LSDA or LSDA+*U*, PBE-GGA or PBE-GGA+*U*, and EV-GGA or EV-GGA+*U* approximations. The electronic structure of AFeO₂ was calculated using the augmented plane wave + local orbital (APW+lo) basis set for 3d electrons and LAPW basic set for s and p electrons. For the atomic spheres, the muffin-tin radii (R_{MT}) were chosen as 1.9, 2.0, and

Table 1. Structural Parameters of AFeO₂

compd	<i>a</i> (Å) ^a	<i>c</i> (Å) ^a	<i>u</i> ^a	<i>u</i> (cal) ^b
CuFeO ₂	3.0351	17.1660	0.1066	0.1057 0.1063 (at $U_{\text{eff}} = 2.18$ eV)
3R-AgFeO ₂	3.0391	18.5900	0.1112	0.1111
2H-AgFeO ₂	3.0391	12.3950	0.0833	0.0835

^a From experiment, refs 1 and 2. ^b From geometry optimization in this work.

1.5 a.u. for Cu, Fe, and O (CuFeO₂) and 2.0, 1.9, and 1.6 for Ag, Fe, and O (AgFeO₂), respectively. Inside the atomic spheres, the partial waves were expanded to $l_{\text{max}} = 10$; the number of plane waves was limited by a cut off $R_{\text{MT}}K_{\text{max}} = 7.0$ for both CuFeO₂ and AgFeO₂. The charge density was Fourier-expanded with $G_{\text{max}} = 14$ Ry. A k-mesh of 1800 k-points in the full Brillouin zone or 182 k points in the irreducible Brillouin zone (IBZ) was used. Convergence was checked up to $R_{\text{MT}}K_{\text{max}} = 9.5$ and 3000 k points in the whole Brillouin zone. In addition to the usual valence states, the following “semi-core” atomic states were considered as being band states: Ag 4s, 4p; Cu 3s, 3p; and Fe 3s, 3p. A ferromagnetic ordering was assumed in all calculations. The AFeO₂ compounds crystallize in the $R\bar{3}m$ structure (see Figure 8a) with the A-atom at 3a (0,0,0), Fe at 3b (0,0,0.5), and O at 6c (0, 0, $\pm u$). The lattice parameters of AFeO₂ were taken from the experiment,¹ whereas the internal parameter *u*, the ratio between the O–A distance and lattice constant *c*, was obtained from geometry optimization within PBE-GGA and PBE-GGA+*U* calculations. A comparison with experimental results¹ is shown in Table 1. The optical properties of AFeO₂ were calculated using the optical module²⁶ in the Wien2k package. This module allows us to study the intra- and direct interband dipole transitions using the joint-density-of-states weighted by the optical dipole matrix elements. The X-ray emission spectra are calculated using the dipole-allowed transitions from the valance to the corresponding core state. The intensities are proportional to the corresponding partial density of states (DOS) times the square of the momentum matrix elements between core and valance states.

III. Band Structures and Optical Properties of CuFeO₂

(a) LSDA and GGA Calculations. The density of states of CuFeO₂ within the LSDA, PBE-GGA, and EV-GGA methods are shown in Figure 1. A metallic state instead of a semiconductor is obtained. The origin of the metallic state of CuFeO₂ comes mainly from the Fe-3d states. The EV-GGA gives the most realistic description, because within the EV-GGA, the top of the valance band and the bottom of the conduction band (mainly due to Fe-3d electrons) overlap only slightly, forming an overlapping band from -0.1 to 0.1 eV around the Fermi level (see Figure 1c). The DOS in Figure 1 show that the Fe ion is in a high-spin state with the spectral weight of Fe-3d spin up band centered slightly below the Cu-3d, but above O-p bands. This is qualitatively in a good agreement with X-ray emission spectra.¹⁹ The calculated X-ray emission spectra of CuFeO₂ within PBE-GGA (the dotted lines) and the EV-GGA (red triangles) are given in Figure 2. Within PBE-GGA, the peak of the Fe–L spectrum is in the energy range of the O–K spectrum and they are 2 eV lower than the peak of the Cu–L spectrum. In comparison with experimental data, we see that the theoretical PBE-

(21) Seshadri, R.; Felser, C.; Thieme, K.; Tremel, W. *Chem. Mater.* **1998**, *10*, 2189.

(22) Ong, K. P.; Bai, K.; Wu, P. *J. Alloys Compd.* **2006**, in press.

(23) Nie, X.; Wei, S. H.; Zhang, S. B. *Phys. Rev. Lett.* **2002**, *88*, 66405.

(24) Engel, E.; Vosko, S. H. *Phys. Rev. A* **1993**, *47*, 2800.

(25) Blaha, P.; Schwarz, K.; Madsen, G. K. H.; Kvasnicka, D.; Luitz, J. *WIEN2k, An Augmented Plane Wave + Local Orbitals Program for Calculating Crystal Properties*; Technical University of Vienna: Vienna, Austria, 2001; ISBN 3-95010.31-1-2.

(26) Abt, R.; Ambrosch-Draxl, C.; Knoll, P. *Physica B* **1994**, 194–196, 1451; Ambrosch-Draxl, C.; Sofo, J. O. *Comp. Phys. Commun.* **2006**, *175*, 1.

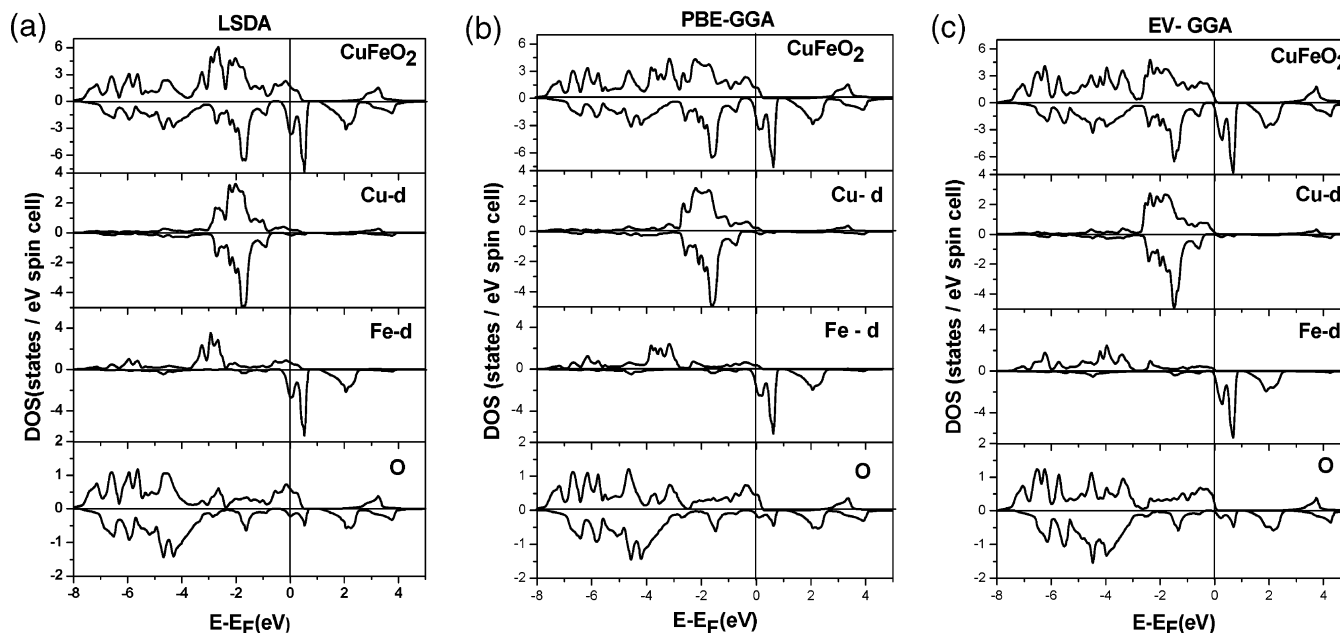


Figure 1. Density of states of CuFeO₂ within different approximations: (a) LSDA, (b) PBE-GGA, and (c) EV-GGA. The positive/negative DOS represents the spin up/spin down DOS, respectively.

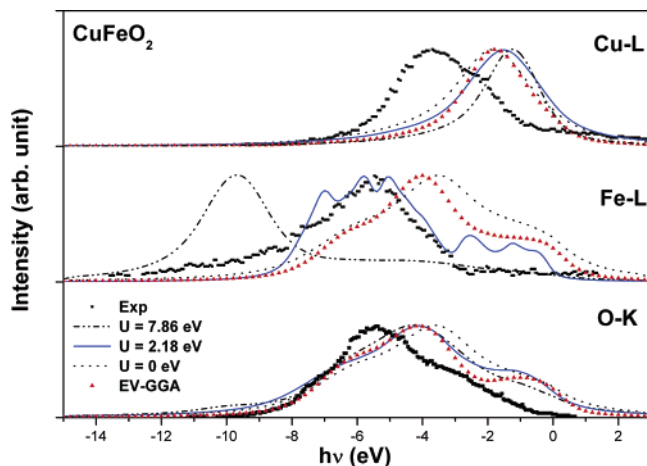


Figure 2. X-ray emission spectra of CuFeO₂ within the EV-GGA and PBE-GGA+*U* using *U* = 0, 2.18, and 7.86 eV. The black squares are experimental data from ref. 19.

GGA Cu–L, Fe–L, and O–K peaks are about 2 eV higher than the experimental data, whereas within the EV-GGA, the theoretical Fe–L and O–K peaks are lowered by 0.6 and 0.7 eV, respectively. Thus the EV-GGA results seem superior to those of PBE-GGA.

Although the band structure calculations within the EV-GGA do not show an energy band gap, the calculated absorption spectra, see Figure 3, start at a finite energy.²⁷ The same phenomenon was observed for CuMoO₂ (M = Al, Ga, In),²³ where the energy band gap is much lower than the optical band gap. This can be explained by the fact that transitions between the top of the valance band (spin up) and the bottom of the conduction band (spin down) are not allowed, following the parity and selection rules.

The spin-polarized absorption spectra (see Figure 3b) show that the experimental optical band gaps,²⁰ $\Delta_0 = 1.15$ and Δ_1

$= 2.03 \pm 0.05$ eV, have their origin from the minority spin states (spindown state), whereas $\Delta_2 = 3.35 \pm 0.1$ eV has its origin from the majority spin (spinup state). The experimental optical gaps are obtained from $(\alpha_{av}h\nu)^2$, and thus we compare directly this quantity (with $\alpha_{av} = (\alpha_{xx} + \alpha_{yy} + \alpha_{zz})/3$). In Figure 4a, an optical gap of $\Delta_0 \approx 1.04$ eV is obtained, which can be compared to $\Delta_0 = 1.15$ eV²⁰ from the experiment. However, the other two experimental optical gaps²⁰ at 2.03 and 3.35 eV cannot be identified from this calculation, where two optical gaps around 2.0 eV (1.80 and 2.20 eV) and two others around 3.3 eV (3.10 and 3.5 eV) are observed. To analyze this, the *xx* and *zz* components of $(\alpha h\nu)^2$ have been plotted in parts b and c of Figure 4c. We can see that gaps at $\Delta_1 = 1.80$ eV and $\Delta_2 \approx 3.10$ eV originate from the *zz* component, whereas the other two theoretical gaps stem from the perpendicular direction.

(b) PBE-GGA+*U* Calculations. The failure of LSDA, PBE-GGA, and EV-GGA calculations in correctly describing the electronic states of CuFeO₂ has its origin in the underestimation of the on-site coulomb correlation between d-electrons of transition-metal ions. The EV-GGA, however, leads to better results for the correlated Fe-3d electrons, but unfortunately, the improvements due to the EV-GGA are not sufficient. Because of this, we have to go beyond GGAs and use a method introducing correlation effects via an external Hubbard *U* parameter, which to some extent is a “fitted” quantity. Once one does this, it is better to use PBE-GGA+*U* instead of EV-GGA+*U*, because PBE-GGA is supposed to be better for the “regular” (noncorrelated) electrons, and the correlated electrons are described anyway via the external *U* parameter. Therefore, we performed calculations by explicitly adding the on-site Coulomb correlation, *U*, with the LSDA+*U* and PBE-GGA+*U* methods.

In a previous report,¹⁹ the 2.0 eV energy band gap was reproduced by taking into account the electron correlation *U* = 8.0 eV and *J* = 0.9 eV for both Cu and Fe. However, we notice here that the X-ray photoelectron core level spectra

(27) We notice here that within the LSDA and PBE-GGA, the absorption spectra of CuFeO₂ start from a finite value at $h\nu = 0$ eV.

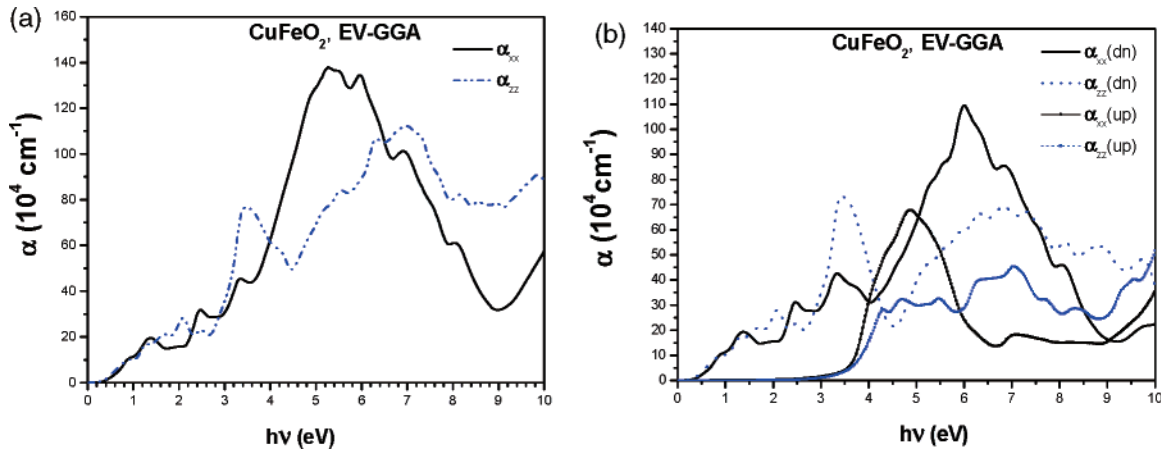


Figure 3. Absorption spectra of CuFeO_2 in perpendicular and parallel directions to the c -axis: (a) the total absorption spectra; (b) the spin polarization absorption spectra.

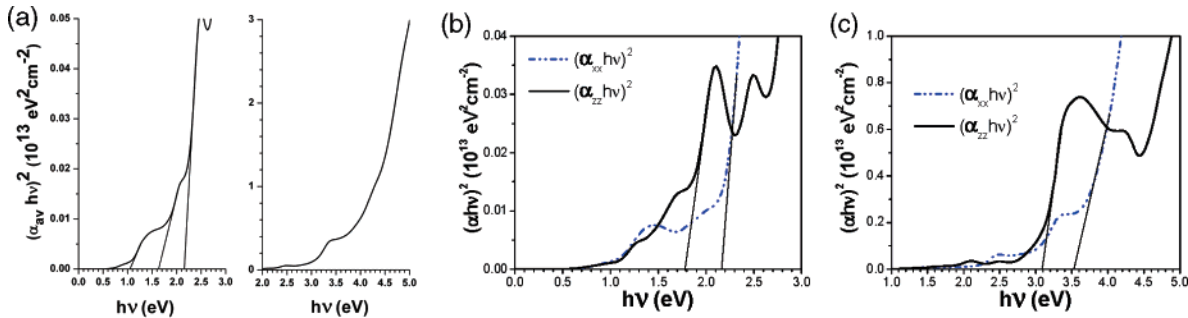


Figure 4. Absorption spectra: (a) $(\alpha_{av}hv)^2$; (b,c) $(\alpha_{xx}hv)^2$ and $(\alpha_{zz}hv)^2$ of CuFeO_2 within the EV-GGA calculation. For demonstration of optical gaps, different scales have been used.

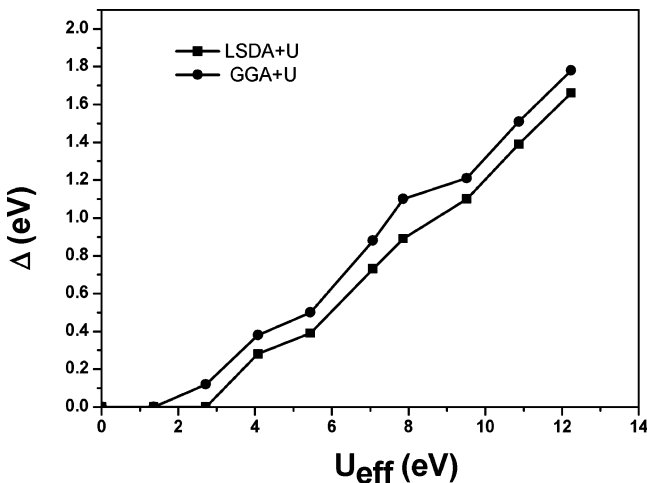


Figure 5. Dependence of energy band gap Δ on the U_{eff} of the CuFeO_2 compound.

on delafossite CuFeO_2 ¹⁹ show that the Cu^+ ion has a closed shell configuration Cu-3d^{10} . As a consequence of this, we will take the on-site coulomb correlation into account for the Fe-3d electrons only. The dependence of the energy band gap, Δ , on U_{eff} ($U_{\text{eff}} = U - J$) is given in Figure 5. Within LSDA+ U and PBE-GGA+ U , an energy band gap will open when $U_{\text{eff}} \geq 2.72$ and 1.36 eV, respectively.

To truthfully describe the band structure of CuFeO_2 , we need to know the value of the effective U_{eff} . In a previous calculation for AgFeO_2 , we obtained $U_{\text{eff}} = 7.86$ eV for the Fe-3d electrons. Because of the similarity of the two systems, CuFeO_2 and AgFeO_2 , we take the same on-site coulomb correlation for Fe-3d electrons for CuFeO_2 . The theoretical

X-ray emission spectra within the PBE-GGA with $U_{\text{eff}} = 7.86$ eV is given in Figure 2 as dash-dot-dot line. The Cu-L and O-K peaks are 2.4 and 1.2 eV higher than the experimental values, whereas the Fe-L peak is 4.2 eV lower. Thus, a value of $U_{\text{eff}} = 7.86$ eV does not really give a good description of the electronic structure of CuFeO_2 and further calculations with significantly reduced U_{eff} were done. At $U_{\text{eff}} = 2.18$ eV, both the theoretical and experimental Fe-L peaks are in good agreement, whereas the Cu-L and O-K peaks are still 2.2 and 1.3 eV higher than the experimental values. From these calculations, we see that U_{eff} for Fe has a strong influence on the Fe-L peak, whereas it has only a minor influence on the Cu-L and O-K peak. Although we do not recommend using U_{eff} for Cu, we notice that applying a large $U_{\text{eff}}(\text{Cu}) = 7.86$ eV for the Cu-3d states leads to the Cu-L peak shifting down by only 1.0 eV, and thus the value is still 1.20 eV higher than that in the experiment.

The above analyses allow us to use $U_{\text{eff}} = 2.18$ eV for Fe, and we optimized the position of the oxygen atoms in CuFeO_2 . We obtained an oxygen position with $u = 0.1063$, see Table 1, which is in very good agreement with the experiment ($u = 0.1066$).

The DOS of CuFeO_2 within PBE-GGA+ U with $U_{\text{eff}} = 2.18$ eV is shown in Figure 6. An energy band gap of 0.29 eV has been obtained, and the character of this gap is predominantly a charge-transfer gap from O-2p to Fe-3d orbitals. The Fe-3d bands have been shifted downward and they overlap significantly with O-2p, so that the O-p DOS also shows some spin-dependency. Almost all minority Fe-3d bands are above the Fermi energy, and thus the Fe^{3+} ions

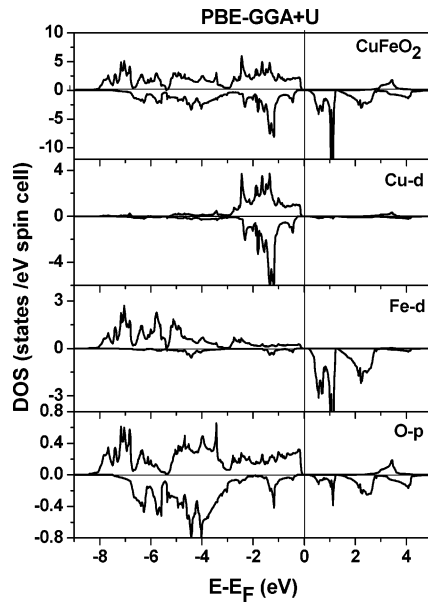


Figure 6. Total and partial density of states of CuFeO_2 within PBE-GGA+ U and $U_{\text{eff}} = 2.18$ eV.

are in a high-spin state. The magnetic moment of the Fe^{3+} ion is $4.1 \mu_B$, which is quite comparable with the $4.2 \pm 0.1 \mu_B$ reported from recent high-resolution neutron powder diffraction experiments¹⁵ but smaller than the $4.4 \mu_B$ obtained from previous powder neutron diffraction experiments²⁸ and the spin moment $5 \mu_B$ obtained from Mossbauer measurements.²⁹ Because of the strong hybridization between Fe and O (and probably due to the assumed FM order), the oxygen atoms also have a significant magnetic moment of $0.28 \mu_B$ (inside the small O-sphere). We notice that within LSDA, PBE-GGA, and EV-GGA calculations, the magnetic moment of Fe^{3+} ion is 3.38 , 3.78 , and $3.98 \mu_B$, respectively. The LSDA value differs a lot from a previous theoretical report¹⁹ that obtained only 0.91 – $0.96 \mu_B$ (a “low-spin” solution) using LMTO-ASA and FP-LAPW methods, respectively. The magnetic moment of the Fe^{3+} ion within EV-GGA comes close to the PBE-GGA+ U results, indicating again that this EV-GGA describes the strong on-site correlation much better than LSDA or PBE-GGA.

The absorption spectra of CuFeO_2 (PBE-GGA+ U calculation) with $U_{\text{eff}} = 2.18$ eV and Lorentzian broadening $\gamma_L = 0.10$ eV are given in Figure 7. The $(\alpha_{\text{av}}/h\nu)^2$ spectrum in Figure 7.b clearly demonstrates an optical gap $\Delta_2 = 3.20$ eV. This gap can be considered as being the direct optical gap $\Delta_2 = 3.35 \pm 0.10$ eV observed from the experiment.²⁰ It has its origin from majority spin in both directions, parallel and perpendicular to the c -axis. At lower energy, two direct optical gaps, $\Delta_0 = 1.30$ and $\Delta_1 = 2.06$ eV, are obtained that are comparable with the experimental indirect optical gap, $\Delta_0 = 1.15 \pm 0.02$ eV, and direct optical gap, $\Delta_1 = 2.03 \pm 0.05$ eV.²⁰ These optical gaps have their origin in transitions due to the minority spin in the direction perpendicular to the c -axis (Δ_1) and in both directions, perpendicular and parallel to the c -axis (Δ_0).

IV. Band Structures and Optical Properties of AgFeO_2

(a) **EV-GGA.** AgFeO_2 has two kinds of polytypes, a rhombohedral structure with space group (Pearson symbol) $R\bar{3}m$ (3R) and a hexagonal structure with $P6_3/mmc$ (2H), as shown in Figure 8. The 3R structure is the same as for CuFeO_2 . In our previous work, the electronic structures within PBE-GGA and LSDA have shown metallic character for 3R and 2H AgFeO_2 .²² The LSDA+ U and GGA+ U calculations gave better results in producing the insulating state of AgFeO_2 with an energy band gap $\Delta = 1.15$ eV at $U_{\text{eff}} \approx 7.86$ eV.²² However, following our analyses in section III for CuFeO_2 , this energy band gap might be overestimated because of the high value of U_{eff} . On the other side, experiments on CuMO_2 and AgMO_2 ($M = \text{Al, Ga, In}$) revealed that the energy band gap of AgMO_2 is larger than that of CuMO_2 .²⁰ Because of this, we might expect that the energy band gap of AgFeO_2 should be larger than that of CuFeO_2 . To clarify this, we have calculated the electronic structure of AgFeO_2 within EV-GGA,²⁴ which is believed to give a better energy band gap than PBE-GGA. Figure 9 shows the DOS of AgFeO_2 within EV-GGA. Contrary to LSDA and PBE-GGA calculations, the EV-GGA calculations result in a small insulating gap, $\Delta \approx 0.05$ eV, for 3R and 2H AgFeO_2 (see Figure 9). In comparison to CuFeO_2 , the

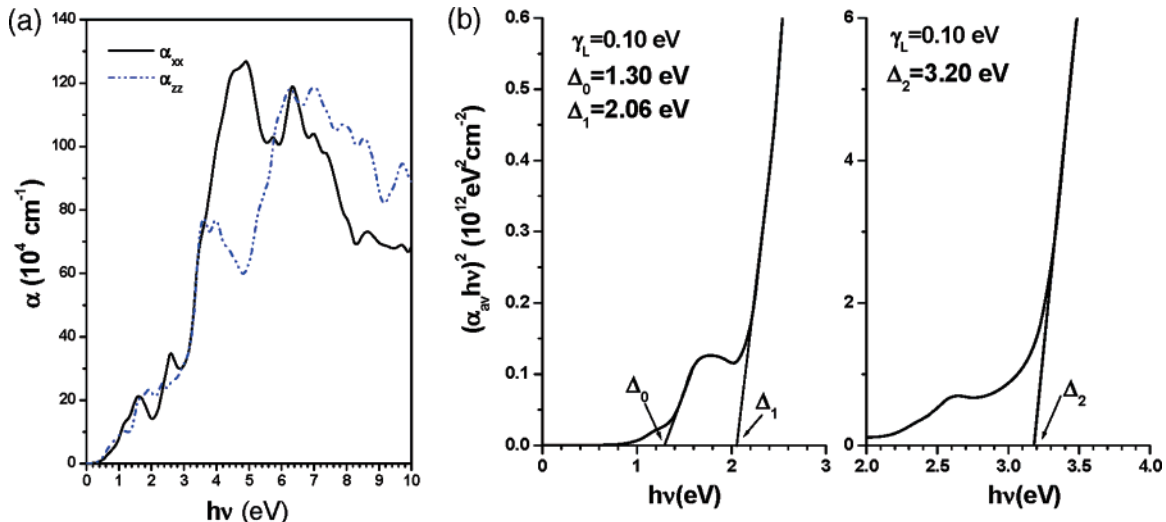


Figure 7. Absorption spectra: (a) α and (b) $(\alpha_{\text{av}}/h\nu)^2$ of CuFeO_2 from PBE-GGA+ U ($U_{\text{eff}} = 2.18$ eV) calculations. For demonstration of optical gaps, different scales have been used.

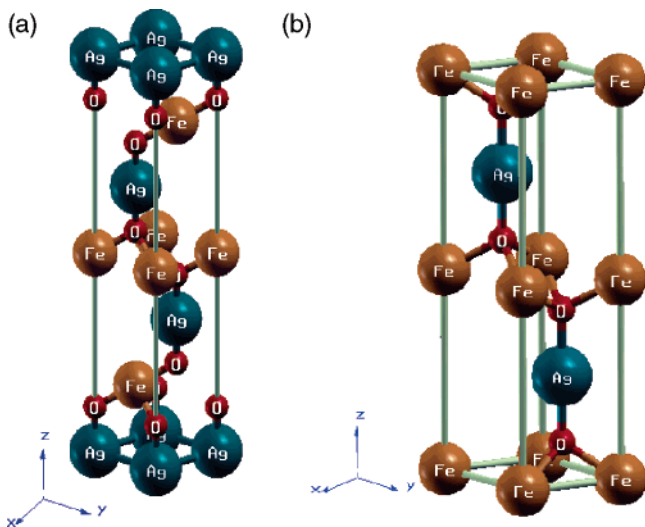


Figure 8. (a) 3R ($R\bar{3}m$) and (b) 2H ($P6_3/mmc$) polytypes of AgFeO_2 .

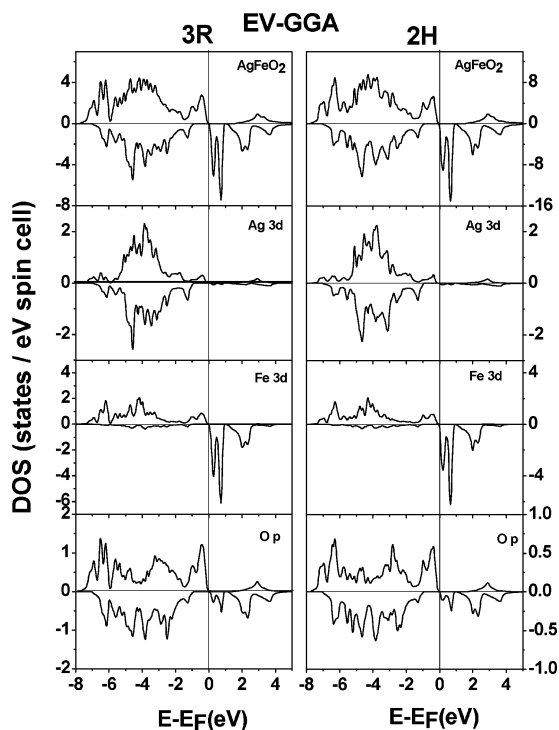


Figure 9. Density of states of 3R- and 2H- AgFeO_2 within the EV-GGA calculation.

Ag-4d states are lower in energy than Cu-3d, and a more pronounced charge-transfer gap character is found.

The absorption spectra of 3R AgFeO_2 are given in Figure 10. It is interesting to see that the tendency that the optical band gap of CuMO_2 is smaller than of AgMO_2 ($M = \text{Al, Ga, In}$) is still true with $M = \text{Fe}$: Within the EV-GGA calculation, one optical gap $\Delta_0 = 1.05$ eV has been obtained for CuFeO_2 , whereas it is $\Delta_0 = 1.7$ eV for 3R AgFeO_2 (the optical gap of 2H AgFeO_2 is not shown here, but has the same value $\Delta_0 = 1.7$ eV).

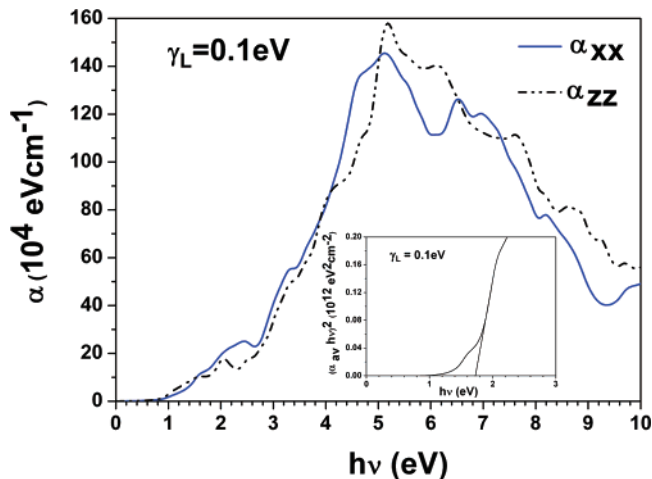


Figure 10. Absorption spectra of 3R- AgFeO_2 within the EV-GGA along the c -axis (α_{zz}) and perpendicular to c (α_{xx}). The inset shows the $(\alpha_{\text{av}}/h\nu)^2$ spectrum with $\alpha_{\text{av}} = (\alpha_{xx} + \alpha_{yy} + \alpha_{zz})/3$, which reveals an optical band gap $\Delta_0 = 1.7$ eV.

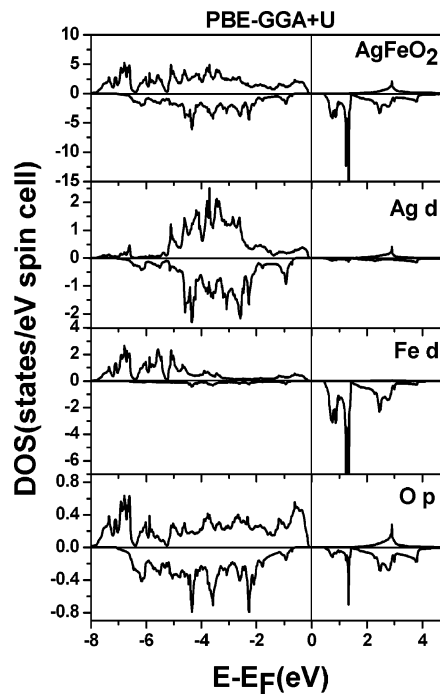


Figure 11. DOS of 3R- AgFeO_2 within PBE-GGA+ U .

(b) PBE-GGA+ U . Although AgFeO_2 is already an insulator within EV-GGA, the strong electron correlation between Fe-3d electrons in AgFeO_2 should not be neglected. Previously, we did calculations of AgFeO_2 within different LSDA+ U and PBE-GGA+ U methods²² using $U_{\text{eff}} = 7.86$ eV, and obtained an energy band gap of 1.15 eV. However, as was mentioned for CuFeO_2 , the effective $U_{\text{eff}} = 7.86$ eV is overestimated, and a smaller $U_{\text{eff}} = 2.18$ eV will be more realistic. Figure 11 shows the corresponding DOS of 3R AgFeO_2 . An energy band gap $\Delta = 0.45$ eV is obtained that has the same nature as CuFeO_2 : It is a charge-transfer gap from O-2p to Fe-3d states.

The absorption spectra in different directions parallel and perpendicular to the c -axis of 3R AgFeO_2 are given in Figure 12. An optical band gap $\Delta_0 \cong 1.9$ eV is obtained (see the inset of Figure 12), which is again larger than the optical band gap $\Delta_0 = 1.2$ eV of CuFeO_2 .

(28) Mekata, M.; Yaguchi, N.; Takagi, T.; Sugino, T.; Mitsuda, S.; Yoshizawa, H.; Hosoito, N.; Shinjo, T. *J. Phys. Soc. Jpn.* **1993**, *62*, 4474.

(29) Muir, A. H.; Wiedersich, J.; Wiedersich, H. *J. Phys. Chem. Solids* **1967**, *28*, 65.

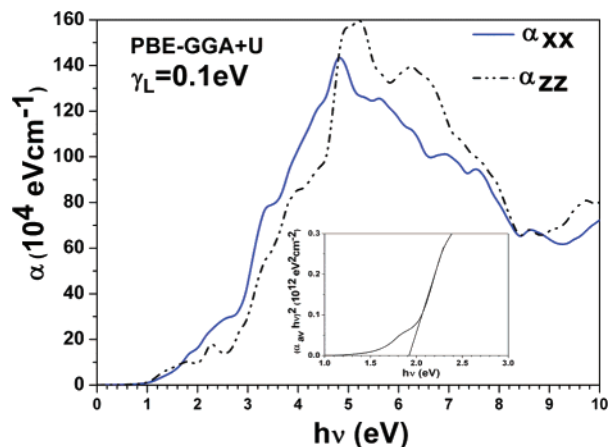


Figure 12. Absorption spectra α_{xx} and α_{zz} of AgFeO_2 within PBE-GGA+ U (and Lorentzian broadening factor $\gamma_L = 0.1$ eV). The inset shows the $(\alpha_0/h\nu)^2$ spectrum, which demonstrates clearly an optical band gap $\Delta_0 = 1.9$ eV.

(c) Origin of Why Optical Band Gap of AgFeO_2 is Larger than That of CuFeO_2 . To understand why AgFeO_2 has a bigger energy band gap than CuFeO_2 , we studied the size effect on the electronic structures of AgFeO_2 and CuFeO_2 using the EV-GGA. When we replace Cu by Ag, keeping the CuFeO_2 crystal structure parameters, the virtual AgFeO_2 compound is metallic. On the other hand, when we replace Ag by Cu using the AgFeO_2 structural parameters, the virtual CuFeO_2 compound is an insulator with an energy band gap of 0.1 eV. These calculations clearly show that the size effect is the primary origin causing the bigger energy band gap in AgFeO_2 than in CuFeO_2 . Larger distances between atoms cause smaller bandwidth and thus larger energy gaps.

IV. Conclusions

In summary, we have studied the electronic structure and optical properties of delafossites CuFeO_2 and AgFeO_2 using different exchange-correlation functionals (LSDA, PBE-GGA, EV-GGA, LSDA+ U , and PBE-GGA+ U). The LSDA and PBE-GGA calculations result in a metallic state that is in contradiction with the semiconducting properties found in the experiment. The EV-GGA describes the semiconducting state of CuFeO_2 and AgFeO_2 better. Within EV-GGA, the AgFeO_2 is a semiconductor with an energy band gap $\Delta = 0.05$ eV, whereas there is still a small band overlap for CuFeO_2 . However, the absorption spectra within EV-GGA reveal an optical gap $\Delta_0 = 1.04$ eV for CuFeO_2 . This can be understood because the transition between the top of the valance band and the bottom of the conduction band is not permitted by parity and selection rules. The EV-GGA

calculations reveal that the experimental optical band gaps of CuFeO_2 , $\Delta_0 = 1.15$ and $\Delta_1 = 2.03 \pm 0.05$ eV, have their origin in the minority spin state, whereas $\Delta_2 = 3.35 \pm 0.10$ eV originates from majority spin states.

The calculated X-ray emission spectra of CuFeO_2 using EV-GGA better agrees with experimental results than those calculated using PBE-GGA. Within the EV-GGA, the theoretical Cu-L, Fe-L, and O-K peaks are 1.90, 1.27, and 1.20 eV higher than the experimental data, respectively.

The role of electron correlations between Fe-3d electrons on the electronic structure and optical properties of CuFeO_2 and AgFeO_2 has been examined using the PBE-GGA+ U method. An effective $U_{\text{eff}} = 7.86$ eV has been obtained from previous ab initio calculations.²² This value seems too large, because the theoretical X-ray emission spectra with this U_{eff} puts the Fe-L peak at 4.2 eV, far below the experimental Fe-L peak, whereas the Cu-L and O-K peaks are nearly unchanged in comparison with PBE-GGA. Exploring different U_{eff} values revealed that $U_{\text{eff}} = 2.18$ eV is a reasonable value in describing the X-ray emission spectra of CuFeO_2 . By using this value, both theoretical and experimental Fe-L peaks are in good agreement, whereas the other theoretical Cu-L and O-K peaks are still 2.2 and 1.3 eV higher than the experimental data, respectively.

The energy band gaps within PBE-GGA+ U of CuFeO_2 and AgFeO_2 are $\Delta = 0.29$ and 0.45 eV, respectively. They are of charge-transfer character from O-2p to Fe-3d states. The absorption spectra of CuFeO_2 reveal three optical band gaps, $\Delta_0 = 1.30$, $\Delta_1 = 2.06$, and $\Delta_2 = 3.20$, which compare well with experimental data, $\Delta_0 = 1.15 \pm 0.02$, $\Delta_1 = 2.03 \pm 0.05$, and $\Delta_2 = 3.35 \pm 0.10$ eV. For AgFeO_2 , an optical band gap $\Delta_0 = 1.90$ eV has been predicted, which is larger than the optical band gap $\Delta_0 = 1.22$ eV of CuFeO_2 . More generally, the conclusions that energy and optical band gaps of CuMO_2 are smaller than those of AgMO_2 for $M = \text{Ga}$, In , Al are also true for $M = \text{Fe}$; this is primarily due to a size effect.

The Fe^{3+} ions in CuFeO_2 are in a high-spin configuration with a magnetic moment of $4.1 \mu_B$, which is in good agreement with the experimentally reported $4.2 \mu_B$. For AgFeO_2 , the magnetic moment of the Fe ions is $\mu(\text{Fe}) = 4.04 \mu_B$.

Acknowledgment. It is a pleasure to thank Dr. Michael Sullivan for critical English proof reading. Financial support from the Institute of High Performance Computing (IHPC) and Agency of Science, Technology, and Research (A*STAR) is gratefully acknowledged. P.B. acknowledges the hospitality of IHPC.

CM062481C